Available online at www.sciencedirect.com
SCIENCE DIRECT®
Journal of Sound and Vibration 264 (2003) 545–557
JOURNAL OF SOUND AND VIBRATION
www.elsevier.com/locate/jsvi

The norms and variances of the Gabor, Morlet and general harmonic wavelet functions

I. Simonovski, M. Boltežar*

Faculty of Mechanical Engineering, University of Ljubljana, Aškerčeva 6, 1000 Ljubljana, Slovenia

Received 19 February 2002; accepted 24 June 2002

Abstract

This paper deals with certain properties of the continuous wavelet transform and wavelet functions. The norms and the spreads in time and frequency of the common Gabor and Morlet wavelet functions are presented. It is shown that the norm of the Morlet wavelet function does not satisfy the normalization condition and that the normalized Morlet wavelet function is identical to the Gabor wavelet function with the parameter $\sigma = 1$.

The general harmonic wavelet function is developed using frequency modulation of the Hanning and Hamming window functions. Several properties of the general harmonic wavelet function are also presented and compared to the Gabor wavelet function. The time and frequency spreads of the general harmonic wavelet function are only slightly higher than the time and frequency spreads of the Gabor wavelet function. However, the general harmonic wavelet function is simpler to use than the Gabor wavelet function. In addition, the general harmonic wavelet function can be constructed in such a way that the zero average condition is truly satisfied. The average value of the Gabor wavelet function can approach a value of zero but it cannot reach it.

When calculating the continuous wavelet transform, errors occur at the start- and the end-time indexes. This is called the edge effect and is caused by the fact that the wavelet transform is calculated from a signal of finite length. In this paper, we propose a method that uses signal mirroring to reduce the errors caused by the edge effect. The success of the proposed method is demonstrated by using a simulated signal.

1. Introduction

In recent years, the wavelet transform [1] has emerged as a powerful new method for monitoring the spectral content of both non-stationary and stationary processes. This transform

*Corresponding author. Tel.: +386-1-4771-608; fax: +386-1-2518-567.
E-mail addresses: igor.simonovski@fs.uni-lj.si (I. Simonovski), miha.boltezar@fs.uni-lj.si (M. Boltežar).

0022-460X/03/$ - see front matter
PII: S0022-460X(02)01206-3

correlates the observed process, $f(t)$, with a family of functions that can be simultaneously translated in time and scaled in the frequency domain. These functions are called wavelets. One major advantage of this method is that one can vary the time–frequency resolution, which allows us to dynamically adapt to the desired time or frequency resolution. In earlier studies, these properties were used to monitor the frequency content of a washing machine during startup [2] and for detecting faults of DC electromotors [3].

This paper deals with certain properties of the wavelet functions that are used for the continuous wavelet transform (CWT). The time and frequency spreads of the wavelet function have to be considered when it is selected, and several parameters of the wavelet functions can affect the conditions (e.g., the zero average value or the norm) that wavelet functions must meet. Additional conditions arise when the CWT is calculated from discrete signals. If one uses approximately analytical wavelet functions, the frequency modulation parameter depends directly on the sampling frequency. These relations are discussed in this paper.

When calculating the CWT, errors occur at the start- and the end-time indexes. This is called the edge effect or the cone of influence [4], and it is caused by the fact that the wavelet transform is calculated from a signal of finite length.

The first part of this paper gives a short introduction to the CWT. The second part deals with the properties of the Gabor, Morlet and general harmonic wavelet functions. The last part of the paper discusses the edge effect.

2. The continuous wavelet transform

The CWT $Wf(u,s)$ of a function $f \in \mathbf{L}^2(\mathbb{R})$ at time u and scale s is defined as [5]:

$$Wf(u,s) = \int_{-\infty}^{+\infty} f(t)\psi^*_{u,s}(t)\,\mathrm{d}t, \tag{1}$$

where * represents a complex conjugation and $\psi_{u,s}(t)$ is created by the translation of a wavelet function $\psi(t)$ by u and a scaling by s, Eq. (2). These two coefficients are called the translation parameter and the scaling factor, respectively. The wavelet function $\psi(t)$ is a function with zero average value, Eq. (3), and is normalized [5], Eq. (4).

$$\psi_{u,s}(t) = \frac{1}{\sqrt{s}}\psi\left(\frac{t-u}{s}\right), \tag{2}$$

$$\int_{-\infty}^{+\infty} \psi(t)\,\mathrm{d}t = 0, \tag{3}$$

$$\|\psi(t)\|^2 = \int_{-\infty}^{+\infty} |\psi(t)|^2\,\mathrm{d}t = 1. \tag{4}$$

The CWT of a function $f \in \mathbf{L}^2(\mathbb{R})$ localizes the signal with a time–frequency window H [6] defined with a Cartesian product, Eq. (5), where $\bar{u}_{u,s}$ and $\bar{\omega}_{u,s}$ stand for the time and frequency centres of the wavelet function that is translated and scaled, Eqs. (6) and (7).

$$H = [\bar{u}_{u,s} \pm \sigma_{t_{u,s}}] \times [\bar{\omega}_{u,s} \pm \sigma_{\omega_{u,s}}], \tag{5}$$

$$\bar{u}_{u,s} = \frac{1}{\|\psi_{u,s}(t)\|^2} \int_{-\infty}^{+\infty} t\,|\psi_{u,s}(t)|^2\,\mathrm{d}t = s\bar{u} + u \quad \text{(see Eq. (A.2))}, \tag{6}$$

$$\bar{\omega}_{u,s} = \frac{1}{2 \cdot \pi \cdot \|\psi_{u,s}(t)\|^2} \cdot \int_{-\infty}^{+\infty} \omega \cdot |\hat{\psi}_{u,s}(\omega)|^2 \cdot \mathrm{d}\omega = \frac{1}{s} \cdot \bar{\omega} \quad \text{(see Eq. (A.4))}. \tag{7}$$

In Eqs. (6) and (7) $\bar{u}$ and $\bar{\omega}$ represent the time and frequency centres of a wavelet function $\psi(t)$, see also Eqs. (A.1) and (A.3). $\hat{\psi}_{u,s}(\omega)$ stands for the integral Fourier transform of the translated and scaled wavelet function $\psi_{u,s}(t)$. The variances of the translated and scaled wavelet function in the time and frequency domains are given by $\sigma^2_{t_{u,s}}$ and $\sigma^2_{\omega_{u,s}}$ as shown:

$$\begin{aligned}
\sigma^2_{t_{u,s}} &= \frac{1}{\|\psi_{u,s}(t)\|^2} \int_{-\infty}^{+\infty} (t - \bar{u}_{u,s})^2 |\psi_{u,s}(t)|^2\,\mathrm{d}t \\
&= 1 \underbrace{\int_{-\infty}^{+\infty} (t - s\bar{u} - u)^2 \left|\psi\left(\frac{t-u}{s}\right)\right|^2 \frac{1}{s}\,\mathrm{d}t}_{\text{new variable } \frac{t-u}{s}=z} \\
&= \int_{-\infty}^{+\infty} (zs + u - s\bar{u} - u)^2 |\psi(z)|^2 \frac{1}{s} s\,\mathrm{d}z \\
&= s^2 \underbrace{\int_{-\infty}^{+\infty} (z - \bar{u})^2 |\psi(z)|^2\,\mathrm{d}z}_{\sigma_t^2} = s^2\sigma_t^2,
\end{aligned} \tag{8}$$

$$\begin{aligned}
\sigma^2_{\omega_{u,s}} &= \frac{1}{2\pi\|\psi_{u,s}(t)\|^2} \int_{-\infty}^{+\infty} (\omega - \bar{\omega}_{u,s})^2 |\hat{\psi}_{u,s}(\omega)|^2\,\mathrm{d}\omega \\
&= \frac{1}{2\pi 1} \underbrace{\int_{-\infty}^{+\infty} \left(\omega - \frac{1}{s}\bar{\omega}\right)^2 |\sqrt{s}\mathrm{e}^{-\mathrm{i}u\omega}\hat{\psi}(s\omega)|^2\,\mathrm{d}\omega}_{\text{new variable } s\cdot\omega=z} \\
&= \frac{1}{2\pi} \int_{-\infty}^{+\infty} \left(\frac{z}{s} - \frac{\bar{\omega}}{s}\right)^2 s|\hat{\psi}(z)|^2 \frac{\mathrm{d}z}{s} \\
&= \frac{1}{s^2} \underbrace{\frac{1}{2\pi} \int_{-\infty}^{+\infty} (z - \bar{\omega})^2 |\hat{\psi}(z)|^2\,\mathrm{d}z}_{\sigma_\omega^2} = \frac{1}{s^2}\sigma_\omega^2.
\end{aligned} \tag{9}$$

3. Wavelet functions

3.1. The Gabor wavelet function

The Gabor wavelet function is obtained by multiplying the Gaussian window by $e^{i\eta t}$, as shown below, where σ defines the width of the wavelet function and $i = \sqrt{-1}$.

$$\psi_{Gabor}(t,\sigma,\eta) = \underbrace{\frac{1}{(\sigma^2\pi)^{1/4}} e^{-t^2/2\sigma^2}}_{Gaussian\ \ window} e^{i\eta t}. \tag{10}$$

The coefficient η depends on the sampling frequency and the selected minimum scale. The Gabor wavelet function belongs to the family of analytical wavelets. The relationship between the scale and the frequency can be obtained from the Fourier integral transform of the translated and scaled Gabor wavelet function $\hat{\psi}_{Gabor_{u,s}}(\omega)$ [7], Eq. (11), or from the frequency centre of the Gabor wavelet function [7], Eq. (12).

$$\hat{\psi}_{Gabor_{u,s}}(\omega) = (4\pi\sigma^2)^{1/4} e^{-i\omega u} e^{-(\omega-\eta/s)^2\sigma^2 s^2/2}, \tag{11}$$

$$\bar{\omega} = \eta \quad \rightarrow \quad \bar{\omega}_{u,s} = \frac{\eta}{s}. \tag{12}$$

The relationship between the scale and the frequency is therefore:

$$\omega = \frac{\eta}{s}, \quad f = \frac{\eta}{2\pi s}. \tag{13}$$

When using discrete signals the Nyquist criterion must be met:

$$f_{max} \leqslant \frac{1}{2\,\Delta t} = \frac{f_s}{2}, \tag{14}$$

where Δt is a time increment and f_s represents the sampling frequency. From Eq. (14) the coefficient η can be calculated as:

$$f_{max} = \frac{\eta}{2\pi s_{min}} \leqslant \frac{1}{2\,\Delta t} \quad \Rightarrow \quad \eta = \frac{s_{min}\pi}{\Delta t}. \tag{15}$$

One should select $s_{min} \geqslant 2$ to avoid undersampling of the wavelet function. In accordance with Eq. (3) the Gabor wavelet function should have an average value of zero. The average value of the Gabor wavelet function is given by expression (16) [7].

$$Average = \int_{-\infty}^{+\infty} \frac{1}{(\sigma^2\pi)^{1/4}} e^{t^2/(2\sigma^2)} e^{i\eta t}\, dt = \sqrt[4]{4\pi\sigma^2}\, e^{-\eta^2\sigma^2/2}. \tag{16}$$

The coefficient η should be large enough so that the average value of the Gabor wavelet function is approximately zero. From expression (16) it follows that if $\sigma = 1.0$ and $\eta \geqslant 5$, then $Average \leqslant 7 \times 10^{-6}$. The parameter s_{min} is chosen with the time and the frequency variances in mind, see Table 1. If a low value for s_{min} is chosen, the time variance at a certain scale s will decrease and the frequency variance at the same scale s will increase. On the other hand, if a high value for s_{min} is chosen, the time variance at a certain scale s will increase and the frequency variance at the same

scale s will decrease. The frequency variance of the Gabor wavelet function is proportional to the frequency ω, while the time variance of the Gabor wavelet function is proportional to $1/\omega$.

3.2. The Morlet wavelet function

The Morlet wavelet function [8,9] is defined as

$$\psi_{Morlet}(t,\eta) = \mathrm{e}^{-t^2/2}\mathrm{e}^{\mathrm{i}\eta t}. \tag{17}$$

The coefficient η depends upon the sampling frequency and the selected minimum scale. It is evident from Eq. (17) that the Morlet wavelet function is basically the Gabor wavelet function with $\sigma = 1$ and without the $1/\sqrt[4]{\pi}$ in the denominator of the Gabor wavelet function, Eq. (10). Table 2 lists the basic properties of the Morlet wavelet function.

$$\|\psi_{Morlet}(t,\eta)\|^2 = \int_{-\infty}^{+\infty} |\mathrm{e}^{-t^2/2}\mathrm{e}^{\mathrm{i}\eta t}|^2 \,\mathrm{d}t = \int_{-\infty}^{+\infty} \mathrm{e}^{-t^2} \,\mathrm{d}t = \sqrt{\pi}. \tag{18}$$

The Morlet wavelet function has to be normalized to comply with the normalization condition, Eq. (4). If the Morlet wavelet function is divided by $1/\sqrt[4]{\pi}$, the normalized Morlet wavelet

Table 1
Properties of certain wavelet functions [7]

Property	Gabor	General harmonic
Average value $\bar{\psi}$	$\sqrt[4]{4\pi\sigma^2}\,\mathrm{e}^{-\eta^2\sigma^2/2}$	$\sin(\eta)\frac{2\pi^2/\sqrt{3}}{\eta(\pi^2-\eta^2)}$
Norm $\|\psi(t,\sigma,\eta)\|^2$	1	1
Time centre $\bar{u}$	0	0
Frequency centre $\bar{\omega}$	η	η
Time spread $\sigma_{t_{u,s}}$	$s\frac{\sigma}{\sqrt{2}}$	$s\sqrt{\frac{2\pi^2-15}{6\pi^2}}$
Frequency spread $\sigma_{\omega_{u,s}}$	$\frac{1}{s}\frac{1}{\sqrt{2}}\frac{1}{\sigma}$	$\frac{1}{s}\frac{\pi}{\sqrt{3}}$
BT product $\sigma^2_{t_{u,s}} \cdot \sigma^2_{\omega_{u,s}}$	$\frac{1}{4}$	$\frac{2\pi^2-15}{6\pi^2}\frac{\pi^2}{3} = 0.2633$
Scale–frequency relationship	$\omega = \frac{\eta}{s}$	$\omega = \frac{\eta}{s}$

Table 2
Properties of the Morlet wavelet function

Property	Value
Average value $\bar{\psi}$	$\mathrm{e}^{-(\eta^2/2)}\sqrt{2\pi}$
Norm $\|\psi(t,\eta)\|^2$	$\sqrt{\pi}$

function is obtained, Eq. (19). However, the normalized Morlet wavelet function is identical to the Gabor wavelet function with the parameter $\sigma = 1$.

$$\psi_{Morlet_{normalized}} = \frac{1}{\sqrt[4]{\pi}} e^{-t^2/2} e^{i\eta t}. \tag{19}$$

3.3. The general harmonic wavelet function

In this part the general harmonic wavelet function is developed. The harmonic wavelet function is well known in the literature. It was developed by Newland in [10–12] and lately used for the analysis of the transient signals [13]. The Fourier integral transform of these wavelets is a constant value in the certain frequency band while outside of this frequency band is equal to zero. A different approach is used for developing the general harmonic wavelet. The Hamming and Hanning window functions are a starting point. The Hamming and Hanning window functions can be defined with Eq. (20), where A and B are constants. For the Hamming window $A = 0.54$, $B = 0.46$ and for the Hanning window $A = B = 0.5$.

$$w_H(t, A, B) = \left\{ \begin{array}{ll} [A + B\cos(\pi t)]: & |t| < 1 \\ 0: & \text{elsewhere} \end{array} \right\}. \tag{20}$$

The general harmonic wavelet function is defined as

$$\psi_{GenHarm}(t, A, B, \eta) = w_H(t, A, B) e^{i\eta t}. \tag{21}$$

From the normalization condition, it follows that $2A^2 + B^2 = 1$, as shown below:

$$\begin{aligned} &\|\psi_{GenHarm}(t, A, B, \eta)\|^2 \\ &\quad = \int_{-1}^{+1} |[A + B\cos(\pi t)] e^{i\eta t}|^2 \, dt \\ &\quad = \int_{-1}^{+1} [A^2 + 2AB\cos(\pi t) + B^2 \cos^2(\pi t)] \, dt \\ &\quad = 2A^2 + B^2 \to 2A^2 + B^2 = 1. \end{aligned} \tag{22}$$

Values for the parameters A and B are calculated from the expression of the variance [7], Eq. (23). In Eq. (23) $\bar{\omega}_{GenHarm}$ represents the frequency centre of the wavelet function, Table 1, and $\hat{\psi}_{GenHarm}(\omega, A, B, \eta)$ represents the Fourier integral transform of the general harmonic wavelet function [7], Eq. (24). From expression (23) it follows that $A = B$ and taking into account expression (22) the solution is obtained as $A = B = 1/\sqrt{3}$. If one was to construct the Hamming or Hanning wavelet functions by frequency modulation of the corresponding window functions, the resulting wavelet functions would have an infinite frequency spread as shown below.

$$\begin{aligned} \sigma^2_{\omega_{GenHarm}} &= \frac{1}{2\pi \|\psi_{GenHarm}(t, A, B, \eta)\|^2} \int_{-\infty}^{+\infty} (\omega - \bar{\omega}_{GenHarm})^2 \, |\hat{\psi}_{GenHarm}(\omega, A, B, \eta)|^2 \, d\omega \\ &= A^2\pi^2 - 2A\pi^2(A - B) + \frac{2(A - B)^2}{\pi} \infty \to A = B, \end{aligned} \tag{23}$$

$$\hat{\psi}_{GenHarm}(\omega, A, B, \eta) = \begin{cases} 2A: & \omega = \eta \\ B: & \omega = \eta \pm \pi \\ \sin(\omega - \eta)\dfrac{2A\pi^2 - 2(\omega-\eta)^2(A-B)}{(\omega-\eta)[\pi^2 - (\omega-\eta)^2]}: & \omega \neq \eta \wedge \omega \neq \eta \pm \pi \end{cases}. \quad (24)$$

As is the case with the Gabor wavelet function, the coefficient η depends on the sampling frequency and the selected minimum scale. The procedure for selecting the coefficient η is the same as the procedure for selecting the coefficient η for the Gabor wavelet function. However, if the parameter η is a multiple of π, the average value of the general harmonic wavelet function is zero, Table 1. This can be achieved if $s_{min} = k\,\Delta t$, $k = 2, 3, \ldots$. The general harmonic wavelet function can, therefore, be constructed in such a way that the zero average condition is truly satisfied. On the other hand, the average value of the Gabor wavelet function can be reduced by increasing the parameter η, but it cannot reach a value of zero. The properties of the general harmonic wavelet function are given in Table 1 and are developed in Ref. [7].

When comparing the Gabor and the general harmonic wavelet functions the width and the height of the wavelet functions should be similar to ensure comparable time and frequency spreads. This can be achieved by equalizing the time or frequency spread. The equivalent $s_{GenHarm}$ can be calculated using the equivalent-time-spread approach, Eq. (25), or the equivalent-frequency-spread approach, Eq. (26).

$$\sigma_{t_{u,s}}^2 = s_{Gabor}^2 \frac{\sigma^2}{2} = s_{GenHarm}^2 \frac{2\pi^2 - 15}{6\pi^2},$$

$$\downarrow$$

$$s_{GenHarm} = s_{Gabor}\pi\sigma\sqrt{\frac{3}{2\pi^2 - 15}}. \quad (25)$$

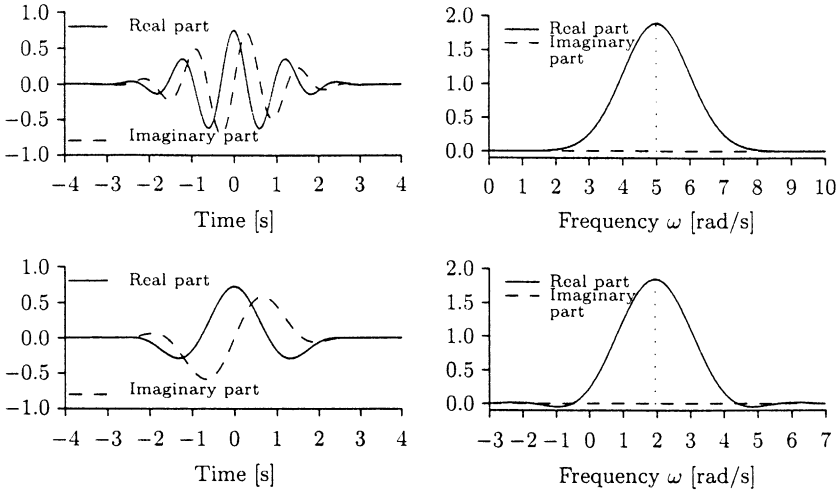

Fig. 1. Gabor (top) and general harmonic (bottom) wavelet function. Parameters of the Gabor wavelet function: $\sigma = 1$, $\eta = 5$, $u = 0$, $s = 1$. Parameters of the general harmonic wavelet function: $A = B = 1/\sqrt{3}$, $\eta = 5$, $u = 0$, $s = 2.565$.

Expressions for the time and frequency spreads are given in Table 1.

$$\sigma^2_{\omega_{u,s}} = \frac{1}{s^2_{Gabor}}\frac{1}{2}\frac{1}{\sigma^2} = \frac{1}{s^2_{GenHarm}}\frac{\pi^2}{3},$$

$$\downarrow$$

$$s_{GenHarm} = s_{Gabor}\pi\sigma\sqrt{\frac{2}{3}}. \tag{26}$$

The Gabor and the general harmonic wavelet functions can, therefore, be compared if the condition specified in expression (27) is satisfied. Fig. 1 shows the Gabor and general harmonic wavelet functions. $s_{GenHarm}$ is calculated using the equivalent frequency spread, Eq. (26).

$$s_{Gabor}\pi\sigma\sqrt{\frac{3}{2\pi^2-15}} \leqslant s_{GenHarm} \leqslant s_{Gabor}\pi\sigma\sqrt{\frac{2}{3}}. \tag{27}$$

4. The edge effect

The CWT is defined with Eq. (1) using the integral limits $(-\infty, +\infty)$. Since the measured signals are of finite length, the CWTs of these signals are affected. Errors occur at the start- and end-time indexes of the calculated CWT. In both regions, a part of the wavelet function is outside the region of the known, measured signal **f**, Fig. 2. When calculating the CWT at the start- and end-time indexes ($u = 0$ and $u = t_{end}$) the measured signal is multiplied by the highest value of the wavelet function. This can cause ripples in the CWT at the start- and end-time indexes, Fig. 5.

Because the width of the wavelet function depends on the scale s, the width of the edge effect also depends on this scale. The edge effect width can be estimated using the time spread $\sigma_{t_{u,s}}$ of the wavelet function. Define the radius of trust R as a multiple k of the time spread of the wavelet

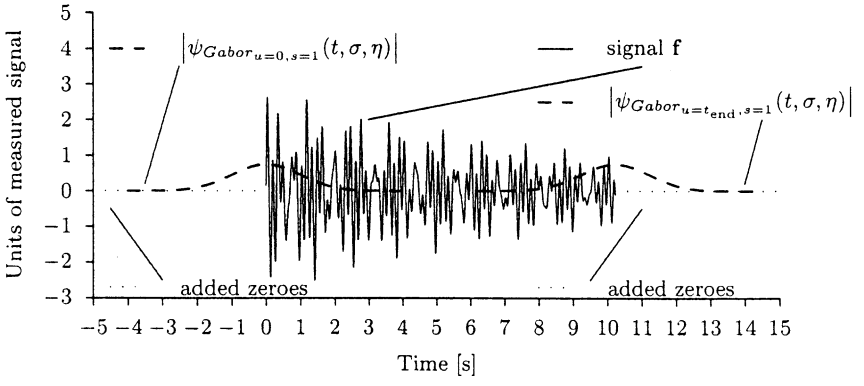

Fig. 2. Edge effect.

function as shown below:

$$R = k\sigma_{t_{u,s}} = ks\sigma_t = k \underbrace{\frac{\eta}{2\pi f}}_{analytical\ \ wavelets} \sigma_t = k\frac{s_{min}}{2f\Delta t}\sigma_t. \tag{28}$$

The area of the calculated CWT affected by the edge effect can be estimated using expression (29). For the Gabor and the general harmonic wavelet functions with the equivalent time spread, the radius of trust is given by expression (30). The parameter η is calculated from Eq. (15). For the general harmonic wavelet function and the equivalent-frequency-spread the radius of trust is given by expression (31). Fig. 3 represents the area of the calculated CWT that is affected by the edge effect. The CWT values at high frequencies are the least affected by the edge effect. However, with a decrease in the frequency the scale increases and, as a result, so does the width of the wavelet function. This is the reason why CWT values are more affected by the edge effect at lower frequencies.

$$t \in [t_{start}, t_{start} + R] \wedge t \in [t_{end} - R, t_{end}], \tag{29}$$

$$R_{Gabor} = ks\frac{\sigma}{\sqrt{2}} = k\frac{\eta}{2\pi f}\frac{\sigma}{\sqrt{2}} = k\frac{s_{min_{Gabor}}}{2f\ \Delta t}\frac{\sigma}{\sqrt{2}}, \tag{30}$$

$$R_{GenHarm} = k\frac{s_{min_{Gabor}}\sigma}{6f\ \Delta t}\sqrt{2\pi^2 - 15} \quad equivalent\ frequency\ spread. \tag{31}$$

Since the general harmonic wavelet function calculated with the equivalent frequency spread has a slightly higher time spread than the Gabor wavelet function, the corresponding area affected by the edge effect is larger. From Fig. 3 one can see that the length of the signal should be longer than the maximum width of the shaded area. The shaded area represents the area of the CWT that is influenced by the edge effect. The minimum required signal length should, therefore, be at least twice R, expression (32). If the signal length is less than $2R$, the low-frequency region of the CWT is significantly influenced by the edge effect.

$$L_{min} \geqslant 2R. \tag{32}$$

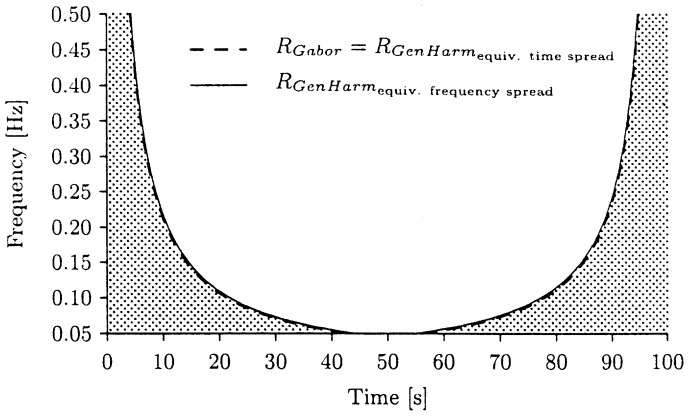

Fig. 3. The area affected by the edge effect. Parameters: $s_{minGabor} = 2$, $\sigma = 1.0$, $\Delta t = 1$ s, $k = 3.0$.

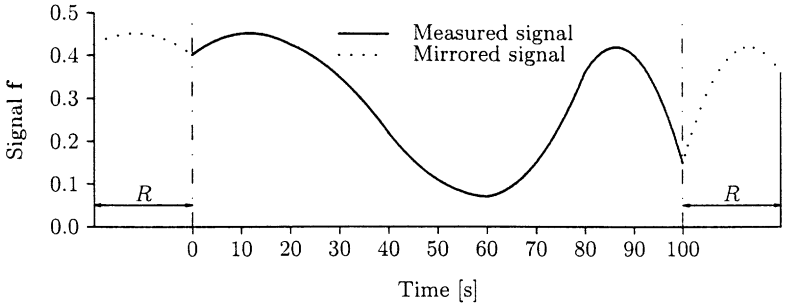

Fig. 4. Mirroring the signal.

Table 3
CWT parameters

Wavelet function	s_{min}	f_{end}	f_{start}	Δf
General harmonic	7.498	0.01 Hz	0.5 Hz	0.005 Hz

The influence of the edge effect can be reduced if the length of the signal is increased by mirroring the signal around the start- and end-time indexes, Fig. 4. The length of the signal is increased by $2R$. R is calculated using Eq. (30) or (31) and the minimum desired calculated frequency. The CWT is then calculated for the lengthened signal. Now the edge effect influences the CWT values at the start- and end-time indexes of the lengthened signal. However, these values can be disregarded because one is only interested in the CWT values corresponding to the time indexes of the original (shorter) signal. Consequently, only the CWT values for the time indexes of the original signal are presented.

An artificial signal, expression (33), was generated for testing the efficiency of the proposed procedure for reducing the edge effect. The signal is composed of two components: the cosines part with constant frequency and amplitude; and a linear chirp of constant amplitude. Using a sampling frequency of $f_s = 1$ Hz we sampled 8192 discrete points of the signal. The parameters used for the CWT calculations are given in Table 3.

$$f(t) = 5\cos(2\pi 0.1t) + \underbrace{5\cos(\pi 3.052\,10^{-5}t^2 + 0.5\pi t)}_{linear\ \ chirp}. \tag{33}$$

Fig. 5 shows the CWT of the signal that was generated with expression (33). In this case no signal mirroring was used. Ripples at the times $t = 0$ and 8191 s can be observed in the frequency ranges of $\sim$0.1 Hz and above 0.3 Hz. These ripples are caused by the edge effect. Fig. 6 shows the CWT of the same signal when signal mirroring was used. The length of the signal was increased by $2R$. R was calculated using $k = 3.0$. The ripples that can be seen in Fig. 5 are no longer present.

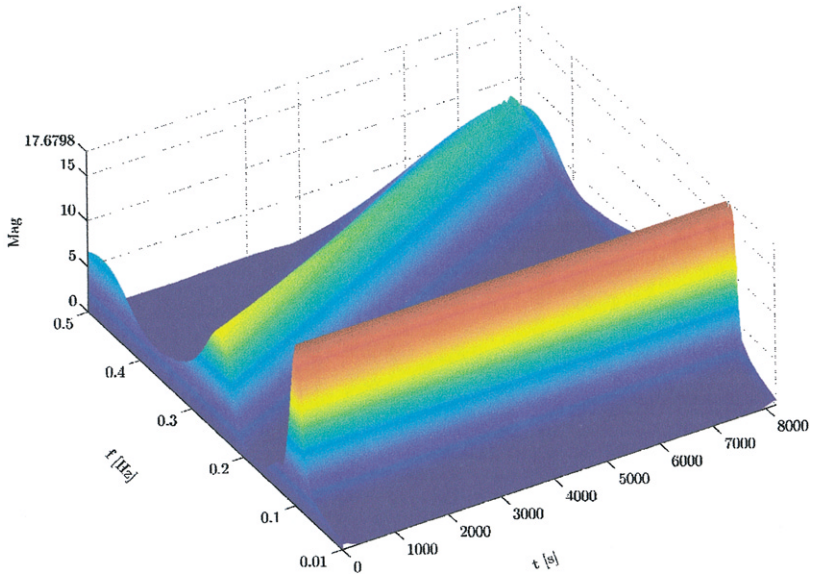

Fig. 5. CWT of generated signal. Ripples at the start- and end-time indexes are visible.

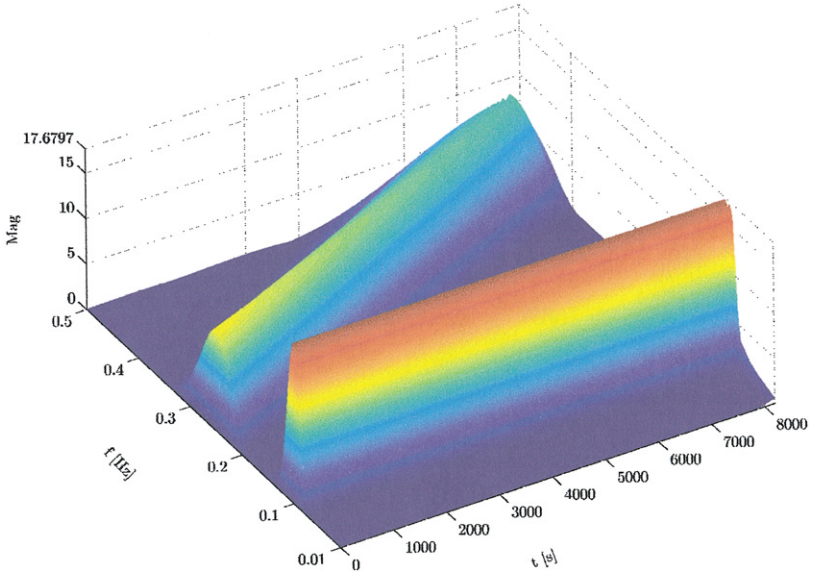

Fig. 6. CWT of generated signal using the procedure for reducing the edge effect. Ripples at the start- and end-time indexes are not visible.

5. Conclusion

This paper deals with certain properties of the continuous wavelet transform and wavelet functions. Specifically, the norms and the spreads in time and frequency of the common Gabor and Morlet wavelet functions are presented. We showed that the norm of the Morlet wavelet

function does not satisfy the normalization condition and that the normalized Morlet wavelet function is identical to the Gabor wavelet function with the parameter $\sigma = 1$.

The general harmonic wavelet function was developed using frequency modulation of the Hanning and Hamming window functions. Several properties of the general harmonic wavelet function are also presented and compared to the well-known Gabor wavelet function. The time and frequency spreads of the general harmonic wavelet function are only slightly higher than the time and frequency spreads of the Gabor wavelet function. However, the general harmonic wavelet function is simpler to use than the Gabor wavelet function. In addition, the general harmonic wavelet function can be constructed in such a way that the zero average condition is truly satisfied. The average value of the Gabor wavelet function can approach a value of zero, but it cannot reach it.

When calculating the continuous wavelet transform, errors occur at the start- and end-time indexes. This is called the edge effect and is caused by the fact that the wavelet transform is calculated from a signal of finite length. In this paper, a method that uses signal mirroring is proposed to reduce the errors caused by the edge effect. The success of the proposed method was shown on a simulated signal.

Acknowledgements

The authors wish to express their gratitude to the Slovenian Ministry of Education, Science and Sport for the financial support through Contract No. S24-782-007/19910/99.

Appendix A

Time centre of the wavelet function:

$$\bar{u} = \frac{1}{||\psi(t)||^2} \int_{-\infty}^{+\infty} t|\psi(t)|^2 \, \mathrm{d}t. \tag{A.1}$$

Time centre of the dilated and scaled wavelet function:

$$\begin{aligned}
\bar{u}_{u,s} &= \frac{1}{||\psi_{u,s}(t)||^2} \int_{-\infty}^{+\infty} t|\psi_{u,s}(t)|^2 \, \mathrm{d}t \\
&= 1 \underbrace{\int_{-\infty}^{+\infty} t\left|\psi\left(\frac{t-u}{s}\right)\right|^2 \frac{1}{s} \, \mathrm{d}t}_{\text{new variable } \frac{t-u}{s}=z} \\
&= \int_{-\infty}^{+\infty} (zs+u)|\psi(z)|^2 \frac{1}{s} s \, \mathrm{d}z \\
&= s \underbrace{\int_{-\infty}^{+\infty} z|\psi(z)|^2 \, \mathrm{d}z}_{\bar{u}} + u \underbrace{\int_{-\infty}^{+\infty} |\psi(z)|^2 \, \mathrm{d}z}_{||\psi(t)||^2=1} = s\bar{u} + u.
\end{aligned} \tag{A.2}$$

Frequency centre of the wavelet function is defined by Eq. (A.3), where $\hat{\psi}(\omega)$ represents the integral Fourier transform of the wavelet function $\psi(t)$.

$$\bar{\omega} = \frac{1}{2\pi||\psi(t)||^2} \int_{-\infty}^{+\infty} \omega|\hat{\psi}(\omega)|^2 \, \mathrm{d}\omega, \tag{A.3}$$

$$\begin{aligned}
\bar{\omega}_{u,s} &= \frac{1}{2\pi||\psi_{u,s}(t)||^2} \int_{-\infty}^{+\infty} \omega|\hat{\psi}_{u,s}(\omega)|^2 \, \mathrm{d}\omega \\
&= \frac{1}{2\pi 1} \int_{-\infty}^{+\infty} \omega|\sqrt{s}\mathrm{e}^{-\mathrm{i}u\omega}\hat{\psi}(s\omega)|^2 \mathrm{d}\omega \\
&= \frac{1}{2\pi} \underbrace{\int_{-\infty}^{+\infty} s\omega|\hat{\psi}(s\omega)|^2 \, \mathrm{d}\omega}_{\text{new variable } s\cdot\omega=z} = \frac{1}{2\pi} \int_{-\infty}^{+\infty} s\frac{z}{s}|\hat{\psi}(z)|^2 \frac{\mathrm{d}z}{s} \\
&= \frac{1}{s} \underbrace{\frac{1}{2\pi} \int_{-\infty}^{+\infty} z|\hat{\psi}(z)|^2 \, \mathrm{d}z}_{\bar{\omega}} = \frac{1}{s}\bar{\omega}.
\end{aligned} \tag{A.4}$$

References

[1] A. Grossman, J. Morlet, Decomposition of hardy function into square integrable wavelets of constant shape, SIAM Journal of Mathematical Analysis and Applications 15 (1984) 723–736.

[2] I. Simonovski, M. Boltežar, Monitoring the instantaneous frequency content of a washing machine during startup, Strojniski vestnik—Journal of Mechanical Engineering 47 (2001) 28–44.

[3] M. Boltežar, I. Simonovski, M. Furlan, Fault detection in dc electro motors using the continuous wavelet transform, Meccanica 38 (2003) 251–264.

[4] C. Torrence, G.P. Compo, A practical guide to wavelet analysis, Bulletin of the American Meteorological Society 79 (1998) 61–78.

[5] S. Mallat, A Wavelet Tour of Signal Processing, 2nd Edition, Academic Press, New York, 1999.

[6] C.K. Chui, An Introduction to Wavelets, Academic Press, New York, 1992.

[7] I. Simonovski, Wavelet Analysis of Non-linear and Non-stationary Vibrations of Electromotor, Ph.D. Thesis, Faculty for Mechanical Engineering, University of Ljubljana, 2002 (in Slovene).

[8] A. Kyprianou, W.J. Staszewski, On the cross wavelet analysis of Duffing oscillator, Journal of Sound and Vibration 228 (1999) 199–210.

[9] J. Lin, Feature extraction of machine sound using wavelet and its application in fault diagnosis, NDT & E International 34 (2001) 25–30.

[10] D.E. Newland, An Introduction to Random Vibrations, Spectral and Wavelet Analysis, 3rd Edition, Addison-Wesley Longman Limited, Harlow, 1993.

[11] D.E. Newland, Wavelet analysis of vibration, part 1: theory, Journal of Vibration and Acoustics 116 (1994) 409–416.

[12] D.E. Newland, Wavelet analysis of vibration, part 2: wavelet maps, Journal of Vibration and Acoustics 116 (1994) 417–425.

[13] D.E. Newland, Ridge and phase identification in the frequency analysis of transient signals by harmonic wavelets, Journal of Vibration and Acoustics 121 (1999) 149–155.